Atmos. Chem. Phys., 14, 7757–7768, 2014
www.atmos-chem-phys.net/14/7757/2014/
doi:10.5194/acp-14-7757-2014

Atmospheric Chemistry and Physics
Open Access

SO_2 noontime-peak phenomenon in the North China Plain

W. Y. Xu[1,3], C. S. Zhao[1], L. Ran[2], W. L. Lin[3,4], P. Yan[3,4], and X. B. Xu[3]

[1]Department of Atmospheric and Oceanic Sciences, School of Physics, Peking University, Beijing, China
[2]Key Laboratory of Middle Atmosphere and Global Environment Observation, Institute of Atmospheric Physics, Chinese Academy of Sciences, Beijing, China
[3]Key Laboratory for Atmospheric Chemistry, Institute of Atmospheric Composition, Chinese Academy of Meteorological Sciences, Beijing, China
[4]Meteorological Observation Center, China Meteorological Administration, Beijing, China

Correspondence to: C. S. Zhao (zcs@pku.edu.cn)

Received: 25 December 2013 – Published in Atmos. Chem. Phys. Discuss.: 4 March 2014
Revised: 30 May 2014 – Accepted: 11 June 2014 – Published: 4 August 2014

Abstract. A phenomenon of frequent noontime SO_2 concentration peaks was discovered in a detailed analysis of the SO_2 concentrations in the North China Plain (NCP). The possible causes and their contributions are analyzed. The impacts of such a phenomenon on the sulphur cycle were studied and the implications of the phenomenon for atmospheric chemistry, cloud physics, and climate were discussed. Different from the more common SO_2 diurnal patterns with high nighttime concentrations, NCP witnessed high frequencies of noontime SO_2 peaks, with an occurrence frequency of 50 to 72 % at four stations. Down mixing of elevated pollution layers, plume transport processes, mountain-valley winds, and fog/high RH haze events were the possible causes. The contribution of each process varies from day to day and from station to station, however, none of those four processes can be neglected. SO_2 peaks occurring during noontime instead of nighttime will lead to a 13 to 35 % increase in sulphur dry deposition, a 9 to 23 % increase in gas phase oxidation, and an 8 to 33 % increase in aqueous phase conversions, which will increase the hygroscopicity and the light scattering of aerosols, thus having important impacts on atmospheric chemistry, cloud physics, and climate.

1 Introduction

High emissions and concentrations of sulphur dioxide (SO_2) have been observed in the North China Plain (NCP) (Lin et al., 2012; Xu et al., 2011b; Zhao et al., 2013), which exerts great impacts on aerosol hygroscopicity and cloud physics (Liu et al., 2011). Yet, the special topography, emission distribution, and meteorological conditions in the NCP have complicated the variation of SO_2 concentrations.

The diurnal variation of primary gas pollutants in polluted regions is typically characterized by morning and evening peaks, due to both the diurnal variations of the planetary boundary layer height (PBLH), emissions, and the diurnal variation in photochemistry (Jacobson, 2002). The SO_2 diurnal variation pattern observed in both the Yangtze River delta region (Wang et al., 2002; Qi et al., 2012) and the Pearl River delta region (Wang et al., 2001), as well as that observed in other parts of the world (Khemani et al., 1987; Psiloglou et al., 2013) seem to mostly comply to this rule, with a few exceptions found by Qi et al. (2012).

The chemical transformation of SO_2 is most rapid during noontime, when the photochemistry is most active and concentrations of oxidants such as the OH radical, H_2O_2 and O_3 are highest (Hua et al., 2008; Ran et al., 2011). OH is the main oxidant for gas phase SO_2 scavenging, while H_2O_2 and O_3 are the major oxidants in aqueous phase SO_2 scavenging processes (Seinfeld and Pandis, 2006). If SO_2 peak values occurred during noontime instead of during nighttime, sulphur conversions would be enhanced, increasing sulphate concentration in aerosols, leading to higher aerosol hygroscopicity and more light scattering.

Adame et al. (2012) reported rare cases of SO_2 peaking during noontime in central southern Spain, which they attributed to transport from industrial regions. Antony Chen et al. (2001) observed a SO_2 noontime peak only in one out of five measurement periods in Maryland (USA), which were

attributed to down-mixing from elevated sources. While this phenomenon seems to be a rare case all over world, several sites in the NCP shows long-term averaged diurnal variation patterns with such variation characteristics (Lin et al., 2011, 2009, 2012, 2008). Short-term observations at both rural and urban sites in the NCP also captured such variation patterns (Gao et al., 2013; Wang, T. et al., 2006). Long-term measurements at rural sites in the Yangtze River delta region also displayed pre-noon SO_2 peaks that were not in accordance with the diurnal variation pattern of other primary gas pollutants (Ding et al., 2013; Qi et al., 2012), however, observations during shorter cam'paigns seem to disagree with these results (Wang et al., 2004). Averaged diurnal patterns usually have large standard deviations due to the high seasonal variability of SO_2 and can be significantly influenced by strong pollution episodes. Thus, the representativeness of such averaged profiles and how common such events are is uncertain. Similarly, their cause or the possible impacts such diurnal variation patterns might have is still not clear. The peak occurrence time at the different type of sites differed from each other, the reason behind that still needs to be found.

In this study, an elaborate investigation into the SO_2 diurnal variation pattern is made based on observations from four stations in the NCP. Possible causes for the noontime peaks and their relative importance are discussed. Finally, the possible impact of such events on the sulphur cycle is investigated and its influence on atmospheric chemistry and climate are pointed out.

2 Data and methodology

2.1 Site and measurements

Measurements of SO_2 and CO (carbon monoxide) were carried out at Wuqing meteorological station (WQ, 39°22′58.8″ N 117°1′1.2″ E, 7.4 m a.s.l) in the NCP during the Haze in China (HaChi) campaign (July 2009 to January 2010). WQ is located in the heart of the plain region and has been proven to be highly representative of the polluted NCP region (Xu et al., 2011a).

Measurements from January 2009 to January 2010 at the Shangdianzi site (SDZ, 40.65° N, 117.12° E; 293.9 m a.s.l.), the China Meteorological Administration site (CMA, 39.95° N, 116.32° E; 96 m a.s.l.) and the Gucheng site (GCH, 39.13° N, 115.12° E; 15.1 m a.s.l.) made by the Chinese Academy of Meteorological Sciences (Lin et al., 2011, 2009, 2012, 2008) were used as references.

Radiosonde data from March 2009 to February 2010 measured at the Nanjiao meteorological station (NJ, 39.8° N, 116.46° E; 33 m a.s.l.) were used to analyze the temperature inversion within the PBLH to better understand the vertical mixing process. The radiosonde measurements were carried out every day at 08:00 LT. The temperature inversion depth of each day was determined and the occurrence frequencies of different inversion depths were counted for spring (March to May 2009), summer (June to August 2009), autumn (September to November 2009), and winter (December 2009 to February 2010), respectively.

The locations of the sites as well as the distribution of SO_2 column concentrations retrieved from the Ozone Monitoring Instrument (OMI) on board AURA satellite (OMSO2Readme file, http://so2.gsfc.nasa.gov/Documentation/OMSO2ReleaseDetails_v111_0303.htm) are shown in Fig. 1.

The SO_2 polluted NCP is surrounded in the north by the Yan Mountains and to the west by the Taihang Mountains. The SDZ, CMA, and GCH sites are aligned along a northeast – southwest line east to the Taihang Mountains, while WQ is about 80 km to the southeast of the CMA site. The SDZ, CMA, GCH, and WQ sites respectively represent the relatively clean background, the polluted urban, rural, and suburban area. SO_2 concentrations are high in the south and relatively lower in the north.

A set of commercial trace gas instruments (Thermo Environmental Instruments Inc., USA C-series) has been used to continuously monitor various trace gases. SO_2 was measured with pulsed UV fluorescence analyzers (TE 43CTL) and CO with gas filter correlation analyzers (TE 48C). Measured gas concentrations were recorded as 1 min average mixing ratios by volume (ppbv), then averaged into 1 h resolutions. Details on the measurements and data calibration can be found in Lin et al. (2012) and Xu et al. (2011b).

2.2 Determination of SO_2 noon-peak phenomenon

Due to the increased emissions, lower boundary layer heights and slower chemical conversions in winter, SO_2 concentrations show significant seasonal variations. In the study of the average SO_2 diurnal pattern, the enhanced signals of wintertime SO_2 data need to be avoided. SO_2 and CO concentrations were divided by the daily maximum value of each day, to acquire the daily normalized diurnal pattern.

Afterwards, patterns with peaks only occurring before 09:00 LT or after 16:00 LT were grouped into the nighttime-peak group (group 1), while patterns of peaks only occurring during 09:00 LT to 16:00 LT were classified into the noontime-peak group (group 2). Diurnal patterns with both a noontime and a nighttime peak during the same day were put into the nighttime & noontime group (group 3). The normalized diurnal variation patterns in each group were averaged and the standard error of the mean ($SEM = \sigma/\sqrt{n}$) was calculated for each hour of the day. The occurrence frequency of each group was calculated for each month of 2009 and for the whole measurement period.

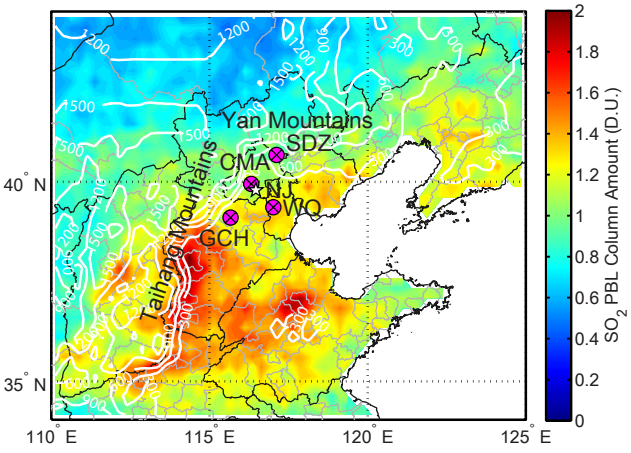

Figure 1. Location of the Shangdianzi (SDZ), China Meteorological Administration (CMA), Gucheng (GCH), Wuqing (WQ) site, the Nanjiao meteorological station (NJ) and the Yan and Taihang Mountains. The average distribution of OMI SO_2 column concentration in 2009 is displayed as the shaded contour, while the white contour lines show the terrain height (m).

2.3 Four possible causes for the SO_2 noon-peak phenomenon

Four possible causes for the SO_2 noontime-peak phenomenon should be evaluated, the down-mixing for elevated SO_2 pollution layers, the transport of plumes, the influence of mountain-valley breezes and the impact of severe haze or fog events. The diurnal SO_2 profiles of group 2 and group 3 were analyzed together with the according CO, wind, RH, and temperature diurnal profiles to determine which of the above four causes has led to the occurrence of the noon peak. Then the contribution of each cause is yielded by dividing the number of noon peak cases caused by a certain factor with the total number of noon peak cases.

If the noon peak was caused by the down-mixing of elevated SO_2 pollution layers, the peak should occur during the early noon time (09:00 to 12:00 LT) when the planetary boundary layer (PBL) is developing. Thus, cases with SO_2 peaks occurring after the morning peak of CO along with the development of the PBL were filed under the down-mixing case category. The development of the PBL is represented by the increase in surface temperature.

CO has a relatively longer lifetime, thus is a very good tracer for pollution plumes. Days with the correlation coefficient between noontime SO_2 and CO reaching a significance level of 95 % were categorized into the plume transport case. Averaged correlation coefficients respectively reached 0.81, 0.82, 0.84, and 0.73 in SDZ, CMA, GCH, and WQ.

Due to the topography of the NCP, all four sites are under the influence of mountain valley circulations, especially the SDZ, CMA, and GCH sites. Winds often change from northern winds to southern ones during noontime (Lin et al., 2009, 2012). SO_2 noontime-peak cases with the above described change in wind direction and with maximum wind speeds below 7 m s^{-1} were counted into the mountain valley breezes case (Chen, 2009).

Severe haze or fog events are characterized by high RH values. For SDZ, GCH, and WQ, the fog or severe haze event is defined as a case with RH exceeding 90 % for over 5 consecutive hours. Since CMA is located in urban Beijing and the site is surrounded by heat sources, RH measured at CMA seldom reaches 90 %. If the RH at CMA exceeds 80 % for over 5 consecutive hours and the other 3 stations simultaneously show RH greater than 90 %, then it is believed that CMA is also experiencing a fog or severe haze event.

2.4 Evaluation of the impacts of the SO_2 noon peak phenomenon on the sulphur cycle

To analyze how the SO_2 diurnal variation pattern influences the sulphur cycle, the WQ site of the HaChi Campaign has been selected to represent the polluted background of the NCP. Normalized SO_2 diurnal variation patterns, which were already grouped based on Sect. 2.2, were averaged respectively for summer (July to August), autumn (September to November), and winter (December to January). The occurrence frequency of each group in each season is calculated. The average SO_2 daily maximum value of each season, which is 20, 40, and 75 ppbv for summer, autumn, and winter, respectively, is multiplied with the average normalized diurnal patterns to yield characteristic SO_2 diurnal concentration variation patterns for the three groups and for each season.

The characteristic SO_2 diurnal concentration variation patterns of the three groups will yield different dry deposition, gas phase oxidation and aqueous phase transformation amounts, which will be compared against each other. The occurrence frequency of the three groups will also be considered to show how the actual diurnal variation pattern influences the sulphur cycle.

2.4.1 The impact on dry deposition

The dry deposition velocity of SO_2 is influenced by the surface type, roughness and the near surface turbulent mixing strength. Surfaces covered by vegetation usually show high SO_2 dry deposition rates during noontime and lower ones during nighttime due to transpiration processes and the strong noontime turbulent mixing processes (Tsai et al., 2010; Raymond et al., 2004). SO_2 concentration peaking during noontime instead of nighttime would increase SO_2 dry deposition fluxes, leading to increased acid depositions.

To study the impact of the SO_2 diurnal variation pattern on dry deposition fluxes, the diurnal variation of the dry deposition velocity v_d measured by Tsai et al. (2010) is used and the dry deposition flux is calculated by

$$F = C \cdot v_d, \quad (1)$$

where C is the SO_2 concentration, which will be provided by the characteristic SO_2 diurnal concentration variation pattern. The dry deposition velocity in the NCP is ranges from 0.2 to 0.8 cm s^{-1}, showing no significant seasonal variations (Pan et al., 2013), which conforms well with the result of Tsai et al. (2010). Thus, it is believed to be appropriate to use the diurnal pattern measured by Tsai et al. (2010) for the NCP region. The total daily dry deposition flux of group 2 and group 3 is compared against that of group 1. The daily dry deposition flux of the three groups are averaged weighted by the occurrence frequency of those three groups and is also compared against that of group 1. This will show how the SO_2 diurnal variation characteristics in the NCP increase the dry depositions compared to the common nighttime-peak pattern observed in other places of the world.

2.4.2 The impact on gaseous oxidation

The NCAR (National Center for Atmospheric Research) Master Mechanism (NCAR-MM version 2.4) photochemical box model is used to calculate the homogeneous diurnal oxidation process of SO_2 (Madronich, 2006; Madronich and Calvert, 1990). The model is coupled with a tropospheric ultraviolet and visible radiation (TUV) model (Madronich and Flocke, 1999), which calculates the photolysis rates needed for photolytic reactions. The radiative properties of the 1 July 2009, 1 October 2009, and 1 January 2010 were modeled to represent the summer, autumn, and winter cases, respectively.

Detailed oxidation processes of SO_2 with various atmospheric oxidants (e.g., OH, O_3, NO_x and organic radicals) are included in the model. The concentration of O_3 and NO_x are constrained according to the seasonally averaged diurnal profiles measured during the Hachi summer campaign, while that of VOCs (Volatile Organic Compounds) could only be constrained according to summertime measurements (Ran et al., 2011). To evaluate the sensitivity of the modeling results to the VOC concentration assumptions, two additional case scenarios with double the amount of summertime VOCs accompanied by half the amount of isoprene and with tripled the amount of summertime VOCs accompanied by a third of the amount of isoprene were calculated. SO_2 concentrations are constrained by the characteristic diurnal variation patterns of the three groups for the three seasons. The entrainment, dilution, and dilution processes have been turned off to focus on the oxidation process.

The daily gas phase oxidized SO_2 amount of group 2 and group 3 is compared against that of group 1. The daily gas phase oxidized SO_2 amount of the three groups are averaged weighted by the occurrence frequency of those three groups and is also compared against that of group 1.

2.4.3 The impact on aqueous oxidation

The SO_2 aqueous oxidation process depends on the atmospheric liquid water content (LWC) as well as the concentration of atmospheric oxidants. For the aqueous phase oxidation of SO_2 the most important two oxidants are H_2O_2 and O_3 (Seinfeld and Pandis, 2006).

The aqueous phase oxidized SO_2 amount can be estimated with the following two equations:

$$\Delta S(\mathrm{IV}) = \left(k_1[\mathrm{SO_2}\cdot\mathrm{H_2O}] + k_2[\mathrm{HSO_3^-}] + k_3[\mathrm{SO_3^{2-}}]\right) \cdot[\mathrm{O_3}]\cdot\Delta t\cdot\mathrm{LWC}\cdot 10^{-6}, \quad (2)$$

$$\Delta S(\mathrm{IV}) = \frac{k_4[\mathrm{H^+}][\mathrm{HSO_3^-}]}{1+k_5[\mathrm{H^+}]}\cdot[\mathrm{H_2O_2}]\cdot\Delta t\cdot\mathrm{LWC}\cdot 10^{-6}, \quad (3)$$

where k_1, …, k_5 are 2.4×10^4 $\mathrm{mol^{-1}\,s^{-1}}$, 3.7×10^5 $\mathrm{mol^{-1}\,s^{-1}}$, 3.7×10^5 $\mathrm{mol^{-1}\,s^{-1}}$, 1.5×10^9 $\mathrm{mol^{-1}\,s^{-1}}$, 7.5×10^7 $\mathrm{mol^{-2}\,s^{-1}}$, 13 $\mathrm{mol^{-1}}$, respectively (Seinfeld and Pandis, 2006). The dissolved concentrations of SO_2, O_3, and H_2O_2 can be calculated with Henry's Law.

Atmospheric LWC exists mostly in clouds, which makes the diurnal variation of atmospheric LWC very complicated. For this study, LWC is assumed to be a constant value 0.029 g m^{-3} throughout the day based on the aircraft measurements of clouds over the NCP (Deng et al., 2009). The pH value is fixed to 5.5 (Sun et al., 2010). The diurnal variation O_3 concentration pattern is set according to Sect. 2.4.2. The H_2O_2 diurnal variation pattern shape is adopted from Hua et al. (2008), due to their relatively long measurement period. The daily maximum H_2O_2 value during summer is set according to measurements in Beijing (He et al., 2010), while those in autumn and winter are set to 0.9 and 0.3 based on the H_2O_2 concentration ratio of autumn / winter to summer in (Sakugawa et al., 1990). The SO_2 concentration pattern is set according to the characteristic diurnal variation patterns of the three groups for the three seasons.

The daily aqueous phase oxidized SO_2 amount of group 2 and group 3 is compared against that of group 1. The occurrence frequency weighting averaged results of the three groups is also compared against that of group 1.

It should be noted that, certain uncertainties will be introduced into this estimation by assuming that trace gas concentrations at cloud level are the same as at ground level. However, the uncertainty will be only shown in the absolute aqueous oxidized amount and will not have influences on the inter-comparison between the groups.

3 Results and Discussions

3.1 SO_2 noontime-peak phenomenon in the NCP

While the SO_2 diurnal variation in other parts of the world were typically characterized by higher values during the

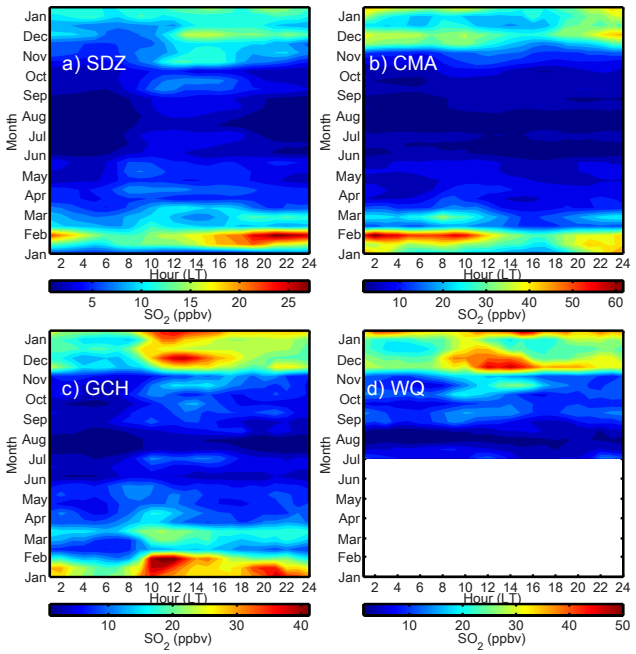

Figure 2. Diurnal and seasonal variation of SO_2 concentrations at the **(a)** Shangdianzi, **(b)** China Meteorological Administration, **(c)** Gucheng and **(d)** Wuqing site.

night and lower ones during the day, this NCP study has revealed a time reversal of SO_2 variation characteristics.

Figure 2a–d displays the season-diurnal variation of SO_2 concentrations at SDZ, CMA, GCH, and WQ, respectively. It can be noted that SO_2 concentrations are usually higher in cold seasons, due to enhanced emissions, weakened removal processes and lower PBLH. Significantly elevated SO_2 values during noontime throughout all the seasons were found at the GCH and WQ stations (Fig. 2c and d). At SDZ, high SO_2 concentrations occur during noontime in all seasons, except for the winter season (Fig. 2a). At CMA, noontime SO_2 peaks could only be observed in spring and autumn, while in winter high SO_2 concentrations occur both during early noon and nighttime (Fig. 2b).

The SO_2 noontime peak seems to be a common phenomenon throughout the NCP region, especially at the WQ and GCH sites, at which the measurements are more representative of the regional background pollution. However, it is still unknown how frequently such events occur, what the causes are and what impacts they may have on atmospheric chemistry, cloud physics, and climate.

For the study of the average diurnal pattern, normalized diurnal patterns were calculated and classified into the nighttime-peak group (group 1), the noontime-peak group (group 2), and the nighttime & noontime group (group 3). The average normalized diurnal variation pattern of each group, the according SEM and the occurrence frequency of each group is displayed in Fig. 3.

As depicted in Fig. 3a1–d1, the total SO_2 noontime-peak occurrence frequency (group 2 + group 3) respectively reached 58%, 50%, 72%, and 69 % at the SDZ, CMA, GCH, and WQ stations. Days with only one noontime peak were more common (SDZ: 43 %, CMA: 31 %, GCH: 47 %, WQ: 44 %), while cases with both noontime and nighttime peaks also often occurred (SDZ: 15 %, CMA: 19 %, GCH: 25 %, WQ: 25 %). At SDZ, GCH, and WQ, the average normalized SO_2 concentration reaches its peak at 00:00 LT, while at CMA the peak occurs between 10:00 to 11:00 LT. The averaged diurnal variation pattern of group 3 shows lower peak values than group 2 and the peaks tend to occur 1 hour earlier than in group 2. However, both group 2 and group 3 for SO_2 reveal distinct noontime peaks.

The averaged diurnal patterns of CO for the CMA, GCH, and WQ sites resemble each other in shape. The normalized CO concentrations of group 2 and group 3 all show peaks at 09:00 LT, which can also be seen as late morning peaks. At SDZ, the CO peak of group 2 occurs between 00:00 LT to 14:00 LT, while that of group 3 is also found between 09:00 to 10:00 LT. The total noontime peak occurrence frequency of CO for SDZ, CMA, GCH, and WQ is 30, 39, 40, and 55 %, respectively.

The total occurrence frequencies of noontime SO_2 peaks in each month for the four stations are listed in Table 1. Distinctly higher occurrence frequencies during warmer seasons were found in SDZ, while in CMA the occurrence frequencies are high in spring and autumn. Noontime-peak occurrence frequencies in GCH show less regular seasonal variations, while those in WQ are relatively lower in summer and higher in autumn and winter.

It can be concluded that, the SO_2 noontime-peak phenomenon occurs frequently at the NCP sites, regardless of seasons. The average peak is mostly reached at 00:00 LT. The highest noontime-peak occurrence frequencies were found at GCH and WQ, the two sites that are most representative of the background pollution state of the NCP. Only a few CO noontime peaks were found and most of them are late morning peaks.

3.2 Causes for SO_2 noontime-peak phenomenon

Different from the SO_2 diurnal patterns in other places of the world, the high SO_2 emissions and concentrations together with the special topography and meteorological characteristics in the NCP have led to a unique noontime-peak pattern. The SO_2 noontime peak could be attributed to four possible causes.

PBL mixing is strongest during noontime, during which down-mixing processes of elevated SO_2 polluted layers will be enhanced. Elevated SO_2 pollution layers could have formed through the emission of stacks whose plumes can rise above the surface temperature inversion layer or through the mountain-chimney effect (Chen et al., 2009), in which surface SO_2 plumes are injected into the free troposphere

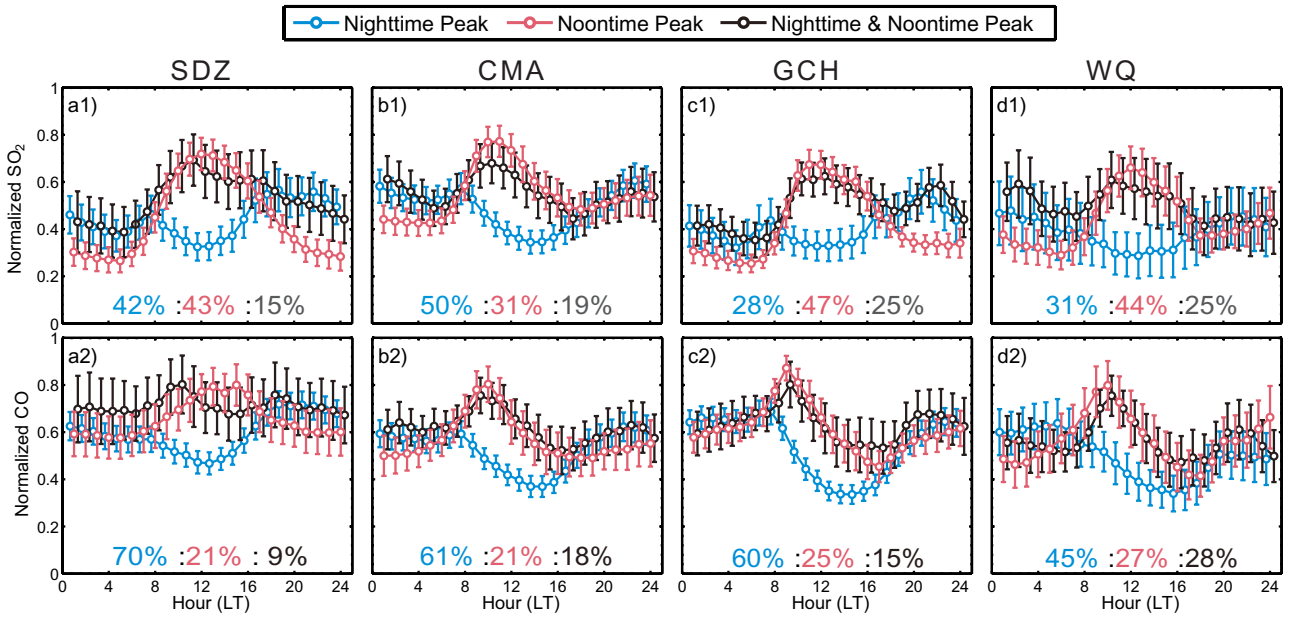

Figure 3. Normalized (1) SO_2 and (2) CO diurnal variation pattern for the days with peaks occurring during nighttime (blue, before 09:00 or after 16:00 LT), noontime (red, between 09:00 and 16:00 LT) and during both nighttime and noontime (black) at **(a)** Shangdianzi, **(b)** China Meteorological Administration, **(c)** Gucheng and **(d)** Wuqing station. The circle and error bar represent the average value ±3 standard error of the mean.

Table 1. Seasonal variation of noontime-peak occurrence frequency

Month	Noontime peak occurrence Frequency (%)			
	SDZ	CMA	GCH	WQ
Jan	39	33	71	–
Feb	32	29	89	–
Mar	26	39	65	–
Apr	33	70	70	–
May	42	47	52	–
Jun	60	50	50	–
Jul	67	32	81	40
Aug	71	55	68	48
Sep	73	67	63	69
Oct	77	58	71	62
Nov	53	52	57	62
Dec	37	16	65	64

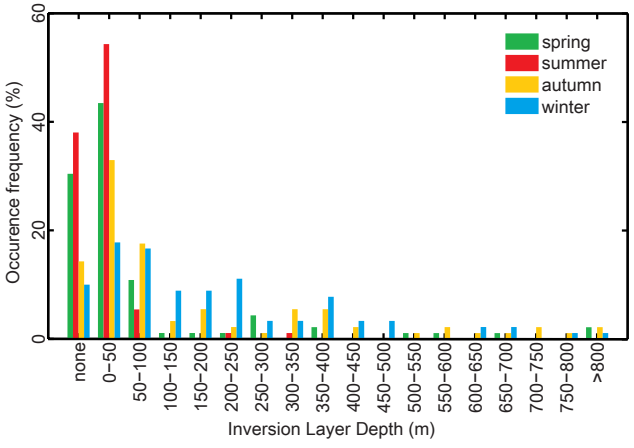

Figure 4. The occurrence frequency of different temperature inversion layer depths during spring (March–May 2009), summer (June–August 2009), autumn (September–November 2009), and winter (December 2009–February 2010) in the 08:00 LT radiosonde data.

through valley winds during the afternoon and transported back to the plain with westerly winds. As is shown in Fig. 4, temperature inversions during 08:.00 LT are most common in autumn and winter, with occurrence frequencies exceeding 80 % of the days. In spring and summer, over 60 % of the days experienced temperature inversions at 08:00 LT. Inversion depth is typically shallow, with 89, 98, 72, and 73 % of the days showing inversion layers depths less than 250 m during spring, summer, autumn, and winter 2009, respectively. Inversion depth is especially shallow in spring and summer, with over 80 and 96 % of the days showing inversion layers below 100 m, respectively. Stacks of industries and power plants are typically 10 to 240 m high and the higher stacks are emitting a significantly larger amount of SO_2 compared to the smaller stacks (Wang, S. et al., 2006; Yang et al., 2008; Zhou et al., 2003). Additionally, due to the plume rise process, the effective plume height could be much higher than the stack heights (Slawson and Csanady, 1971). Thus, the frequent occurrence of shallow inversions together with

Table 2. SO_2 noontime peak occurrence frequency and the fraction of noontime peaks caused by (a) down-mixing due to PBL processes, (b) plume transport, (c) mountain valley breezes, and (d) fog, or severe haze events.

Station	SDZ	CMA	GCH	WQ
Total Sample Count	356	374	395	180
Noontime peak sample count (occurrence frequency)	179 (50 %)	165 (44 %)	269 (68 %)	105 (58 %)
(a) Down-mixing caused noontime peak sample count	60 (34 %)	50 (30 %)	117 (43 %)	55 (52 %)
(b) Plume transport caused noontime peak sample count	38 (21 %)	76 (46 %)	53 (20 %)	31 (30 %)
(c) Mountain Valley Breeze caused noontime peak sample count	72 (40 %)	33 (20 %)	53 (20 %)	6 (6 %)
(d) Fog or severe haze events caused noontime peak sample Count	9 (5 %)	6 (4 %)	49 (18 %)	13 (12 %)

the large amount of SO_2 that is released from higher stacks will favor the formation of elevated SO_2 pollution layers. The average normalized SO_2, CO and temperature profiles that were filed under the down-mixing case category are displayed in Fig. 5a1–a4. Down-mixing case samples take up 34, 30, 43 and 52 % of the noontime peaks at SDZ, CMA, GCH, and WQ, respectively (Table 2a).

The transport of SO_2 plumes can result in sudden increases of local SO_2 concentrations. The plume transport process is characterized by the coherent variation of SO_2 and CO. The average normalized SO_2, CO, and temperature profiles in the plume transport case can be seen in Fig. 5b1–b4. Although SO_2 shows a peak between 09:00 and 12:00 LT, the occurrence time of the peaks caused by plume transport processes was rather random. This process respectively explains 21, 46, 20, and 30 % of the noontime peaks at SDZ, CMA, GCH, and WQ (Table 2b). It should be noted that, due to our classification method, cases with SO_2, and CO both having a late morning peak are also included into this category.

Mountain valley circulations lead to diurnal variations in wind directions, thus resulting in a diurnal variation in pollutant transport. Due to the topography of the NCP, all four sites are under the influence of mountain valley circulations, especially the SDZ, CMA, and GCH sites. Winds often change from northern winds to southern ones during noontime. Due to the stronger SO_2 emissions and resulting higher concentrations in the southern part of the NCP (Fig. 5), southern winds will aid the transport of polluted air masses to our stations. The average diurnal patterns in the mountain valley breezes case are shown in Fig. 5a3–d3. A change in wind direction takes place between 08:00 to 00:00 LT, while SO_2 starts increasing before noon and reaches its peak between 00:00 and 16:00 LT at all four stations. As can be seen in Table 2c, the mountain valley breeze factor can respectively explain 40, 20, 20 and 6 % of the noontime peaks occurring in SDZ, CMA, GCH, and WQ. Since SDZ is a relatively clean background site, the mountain-valley breeze will not only cause increasing noontime SO_2 concentrations but also increasing CO concentrations. This explains why only the SDZ site showed noontime CO peaks in Fig. 3.

Aerosol and fog liquid water can serve as an efficient sink for SO_2. SO_2 is a soluble gas, which can be scavenged effectively through aqueous phase reactions in fog or wet aerosol particles (Pandis et al., 1992). Fog and high RH haze events usually occur during nighttime and persist until the temperature rises up in the morning, leading to low nighttime SO_2 concentrations. Additionally, such events are typically characterized by surface temperature inversions, which will prevent the down-mixing of elevated SO_2 emissions (Jacobson, 2002). With the increasing temperature in the morning, the RH will decrease, weakening the SO_2 scavenging process. The temperature inversion will vanish, allowing for the down-mixing of SO_2 from aloft. Averaged normalized SO_2, CO, and RH profiles in the fog or severe haze case are shown in Fig. 5d1–d4. SO_2 peaks were reached typically between 00:00 and 16:00 LT, depending on how long the fog or high RH event lasted. Such events caused 5, 4, 18 and 12 % of the noontime peak events at SDZ, CMA, GCH, and WQ, respectively.

3.3 Impacts of SO_2 noontime-peak phenomenon on the sulphur cycle

SO_2 peaks occurring during noontime instead of nighttime might have remarkable impacts on human health, environment, and climate. Higher SO_2 concentrations during daytime will not only pose higher health risks for humans, but also change the sulphur cycle.

For surfaces covered with vegetation, dry deposition processes are typically most dynamic during noontime due to transpiration processes and the strong turbulent mixing processes (Raymond et al., 2004; Tsai et al., 2010), thus noontime SO_2 peaks may create more acid deposition than common nighttime peak variation patterns. The calculated diurnal dry deposition fluxes based on the diurnal dry deposition velocity in Tsai et al. (2010) and the characteristic SO_2 diurnal variations of the three groups in WQ during autumn are shown in Fig. 6. Groups 2 and 3 show significantly higher dry deposition fluxes than group 1 during 08:00 to 18:00 LT, while for the other time periods the dry deposition fluxes of the three groups are similar to one another. The estimated daily deposition fluxes for summer, winter and autumn in WQ are listed in Table 4. Seasonally, dry deposition fluxes are higher during colder seasons than during warmer ones, due to elevated SO_2 concentrations, and due to the fact that seasonal variations in dry deposition rates were not considered. Within the same season, the occurrence time of the SO_2 peak had major impacts on the daily dry deposition fluxes. The results of group 2 show a 22 to 46 % increase in daily dry deposition flux compared to those of group 1, while those of

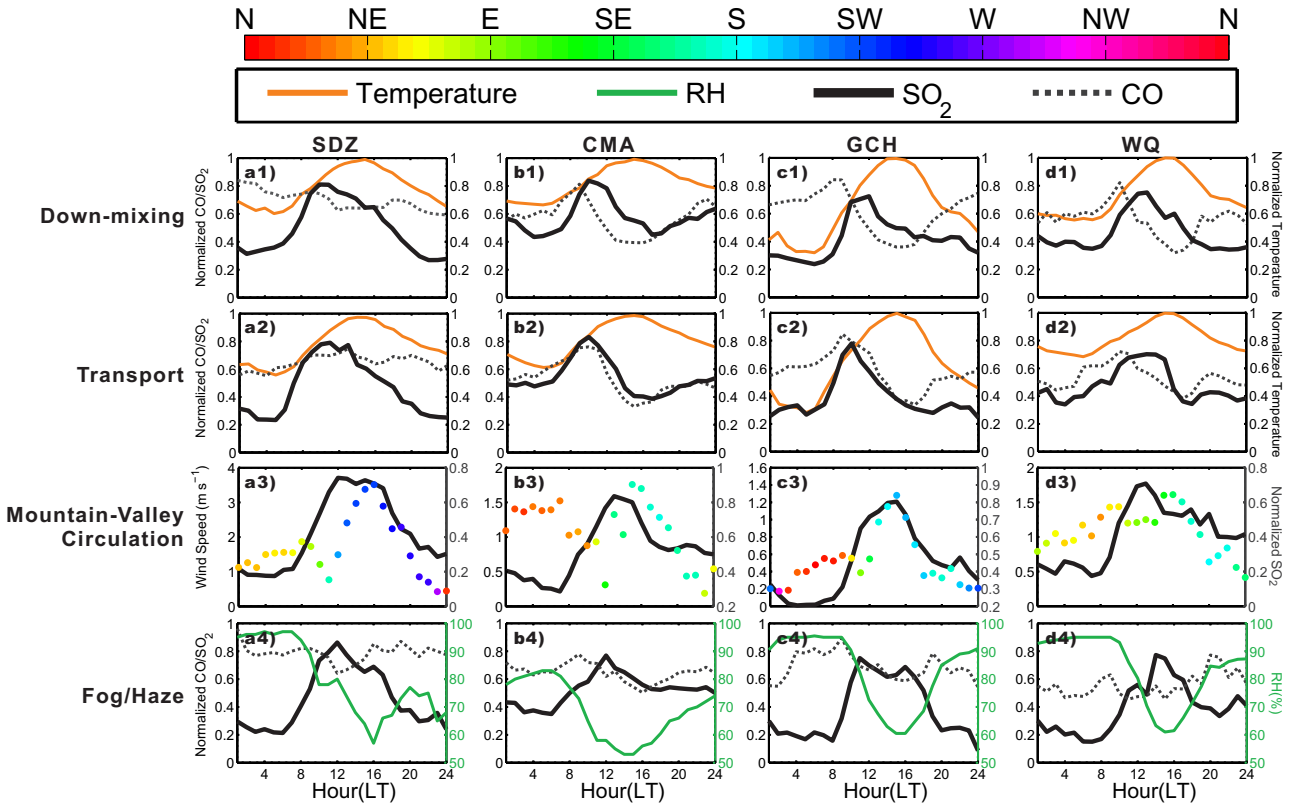

Figure 5. Averaged diurnal variation patterns for (1) the PBL down-mixing, (2) the plume transport, (3) the mountain valley breeze, and (4) the fog/haze case for **(a)** Shangdianzi, **(b)** China Meteorological Administration, **(c)** Gucheng and **(d)** Wuqing.

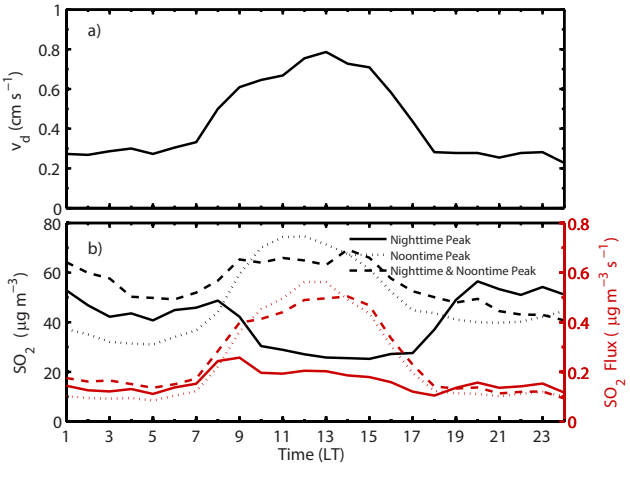

Figure 6. (a) Diurnal variation of the dry deposition velocity inferred from Tsai et al. (2010); **(b)** Calculated dry deposition fluxes (red lines) based on the three characteristic SO_2 diurnal variation patterns (black lines) in Wuqing during autumn 2009.

group 3 show a 44 to 62 % increase. Considering the occurrence frequency of the three diurnal patterns, the weighting averaged daily dry deposition fluxes show increases of 13 to 35 % relative to the common nighttime-peak case, with the lowest increase occurring during summer and the highest one during autumn.

Atmospheric photochemistry is most active during noontime due to favorable radiative conditions. The simulated SO_2 gas phase conversion processes for the three SO_2 diurnal variation patterns in WQ during autumn are displayed in Fig. 7. Due to the fact that deposition processes have been turned off in the simulations, S(VI) products will accumulate in the air parcel. Accumulated S(VI) concentrations of group 3 are the highest throughout the day, while that of group 2 exceeds that of group 1 after 10:00 LT. The SO_2 oxidation rates of group 2 and 3 during noontime are significantly higher than those of group 1. The simulated daily gas phase SO_2 conversion amount for summer, winter, and autumn in WQ are listed in Table 4. Despite the weakened photochemistry during winter, the high SO_2 concentration in winter has led to higher gas phase oxidized SO_2 amounts than in summer. SO_2 noontime-peak patterns could also increase the daily gas phase oxidized SO_2 amount. The results of group 2 show a 15 to 26 % increase in gas phase oxidized amount compared to those of group 1, while those of group 3 show a 28 to 50 % increase. Considering the occurrence frequency of the three diurnal patterns, the weighting averaged gas phase oxidized amounts show increases of 9 to 23 % relative to the common nighttime peak case, with the

Table 3. Estimated SO_2 dry deposition flux for the three different SO_2 diurnal variation patterns, the occurrence frequency (of the three groups) weighting averaged value, and the relative increase compared to the nighttime peak case.

Case	SO_2 dry deposition flux ($g\,m^{-2}\,day^{-1}$) [Increase relative to nighttime peak case (%)]		
	Summer	Autumn	Winter
Nighttime peak	0.0065	0.014	0.028
Noontime peak	0.0079 (22 %)	0.020 (46 %)	0.035 (27 %)
Nighttime + Noontime peak	0.0093 (44 %)	0.022 (58 %)	0.045 (62 %)
Weighting average	0.0073 (13 %)	0.019 (35 %)	0.035 (28 %)

Table 4. Simulated SO_2 gaseous oxidation amount for the three different SO_2 diurnal variation patterns, the occurrence frequency (of the three groups) weighting averaged value, and the relative increase compared to the nighttime peak case. Case 1, case 2, and case 3 respectively represent cases using summertime VOC concentrations, doubled summertime VOC concentrations with half of the summertime isoprene concentrations, and tripled summertime VOC concentrations with a third of the summertime isoprene concentrations.

Case	SO_2 gaseous oxidized amount ($ppbv\,day^{-1}$) [Increase relative to nighttime peak case (%)]						
	summer	autumn			winter		
	Case 1	Case 1	Case 2	Case 3	Case 1	Case 2	Case 3
Nighttime	2.3	3.1	3.7	4.0	3.0	4.0	4.5
Noontime	2.6	3.9	4.6	4.8	3.7	4.7	5.2
	(15 %)	(26 %)	(23 %)	(21 %)	(23 %)	(18 %)	(16 %)
Noontime + Nighttime	2.9	4.3	5.1	5.4	4.5	5.9	6.7
	(28 %)	(39 %)	(36 %)	(35 %)	(50 %)	(49 %)	(49 %)
Weighting Average	2.5	3.8	4.5	4.7	3.7	4.8	5.4
	(9 %)	(21 %)	(19 %)	(19 %)	(23 %)	(21 %)	(20 %)

lowest increase occurring during summer and the highest one in winter. Increased VOC concentrations during autumn and winter will lead to increased SO_2 oxidized amounts, however, the relative increase of group 2 and group 3 to that of group 1 decreases slightly with increasing VOC concentrations. Overall, the VOC concentrations have little influence in the intercomparison between the three groups.

Concentrations of atmospheric oxidants that are important in SO_2 aqueous phase reactions also reach their peaks during noontime. Assuming a constant LWC throughout the day and assuming that concentrations near clouds are similar to the surface concentrations, the estimated SO_2 aqueous phase conversion rate for the three SO_2 diurnal variation patterns in WQ during autumn are displayed Figure 8. SO_2 conversion amounts of group 2 and 3 are significantly higher than those of group 1 during 08:00 to 18:00 LT, with that of group 2 being highest between 11:00 to 16:00 LT. The simulated daily aqueous phase SO_2 conversion amount for summer, winter, and autumn in WQ are listed in Table 4. The aqueous phase scavenged SO_2 amounts during the three seasons are on the same level. The high SO_2 concentrations in winter have been canceled out by the low concentrations in oxidants. The diurnal variation pattern however had much impact on the aqueous phase oxidized SO_2 amount. Compared to group 1, group 2 shows a 13 to 43 % increase in aqueous phase conversion amount, while group 3 shows a 28 to 61 % increase. Considering the occurrence frequency of the three diurnal patterns, the weighting averaged aqueous phase SO_2 conversion amounts show increases of 8 to 33 % relative to the common nighttime-peak case, with the lowest increase occurring during summer and the highest one during autumn.

In all, compared to the nighttime SO_2-peak case, which was observed all around the world, the NCP experienced enhanced sulphur dry depositions and sulphur to sulphate conversions due to the frequently occurring SO_2 noontime peak phenomenon. More acidic deposition is formed. Aerosols in the NCP will show higher sulphate fractions and become more hygroscopic (Liu et al., 2013). This will promote the light scattering effect of aerosols and thus may have important impacts on regional climate.

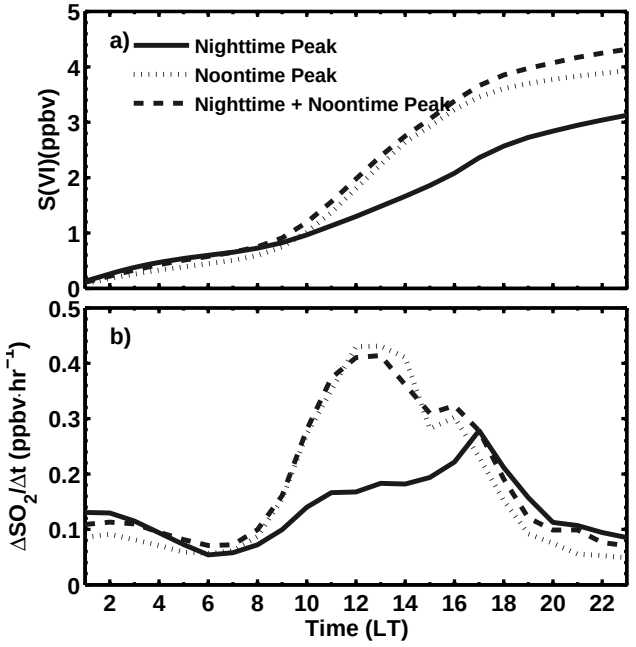

Figure 7. Simulated gas phase oxidized SO_2 **(a)** amount and **(b)** oxidation rates based on the three characteristic SO_2 diurnal variation patterns in Wuqing during autumn 2009.

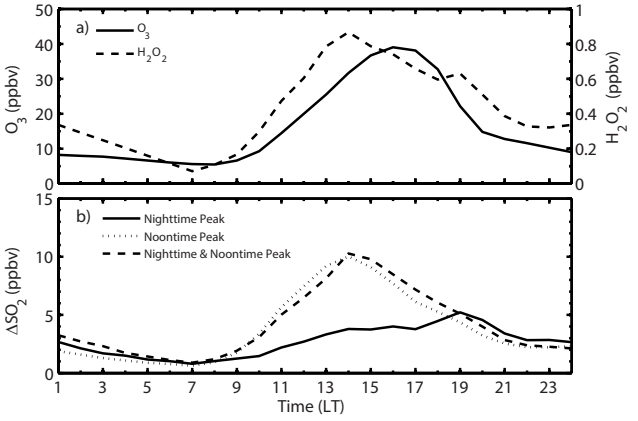

Figure 8. (a) O_3 and H_2O_2 diurnal profiles used in the estimations; **(b)** Estimated aqueous phase oxidized SO_2 amount based on the three characteristic SO_2 diurnal variation patterns in Wuqing during autumn 2009.

Table 5. Estimated SO_2 aqueous oxidation amount for the three different SO_2 diurnal variation patterns, the occurrence frequency (of the three groups) weighting averaged value and the relative increase compared to the nighttime peak case.

Case	SO_2 aqueous oxidized amount (ppbv day^{-1}) [Increase relative to nighttime peak case (%)]		
	Summer	Autumn	Winter
Nighttime Peak	86.5	64.2	62.4
Noontime Peak	97.5 (13 %)	91.6 (43 %)	77.2 (24 %)
Nighttime + Noontime Peak	110.9 (28 %)	99.7 (55 %)	100.6 (61 %)
Weighting average	93.3 (8 %)	85.5 (33 %)	78.8 (26 %)

4 Summary

In this paper, a frequently occurring SO_2 noontime peak pattern was found in the NCP. A detailed analysis of this SO_2 diurnal pattern, the causes for such a phenomenon, and the potential impacts of the phenomenon on the sulphur cycle were investigated.

The total noontime peak occurrence frequency reaches 68, 50, 72, and 69 % in SDZ, CMA, GCH, and WQ, respectively. Down-mixing of elevated pollution layers, plume transport processes, mountain-valley winds and fog/high RH haze events were the possible causes. The contribution of each process varies from each other and from station to station, which the down-mixing process being the most important process at three out of four stations. However, none of those four processes is negligible. The different occurrence frequencies of noontime peak phenomenon and the different contribution of each process to each site has led to distinct noontime peak occurrence times in the long-term averaged diurnal profiles at the different types of sites.

The SO_2 noontime peak phenomenon significantly speeds up the sulphur cycle. Compared to the nighttime SO_2 peak case, which was observed all around the world, WQ respectively experienced 13 to 35 %, 9 to 23 %, and 8 to 33 % enhancement in sulphur dry depositions, gas phase oxidations, and aqueous phase conversions due to the frequently occurring SO_2 noontime peak phenomenon.

SO_2 peaks occurring during noontime instead of nighttime has led to more acidic deposition. Aerosols in the NCP will show higher sulphate fractions and become more hygroscopic. This will promote the light scattering effect of aerosols and thus may have important impacts on regional climate. Higher SO_2 concentrations during daytime will also pose higher health risks for human. The potential impacts of such a phenomenon on human health, environment, and climate should be studied in detail in the future.

Acknowledgements. This work is supported by the National 973 project of China (2011CB403402), National Natural Science Foundation of China (41375134), Beijing Natural Science Foundation (8131003) and the Basic Research Fund of Chinese Academy of Meteorological Sciences (2011Z003).

Edited by: D. Covert

References

Adame, J. A., Notario, A., Villanueva, F., and Albaladejo, J.: Application of cluster analysis to surface ozone, NO_2 and SO_2 daily patterns in an industrial area in Central-Southern Spain measured with a DOAS system, Sci. Total Environ., 429, 281–291, doi:10.1016/j.scitotenv.2012.04.032, 2012.

Antony Chen, L. W., Doddridge, B. G., Dickerson, R. R., Chow, J. C., Mueller, P. K., Quinn, J., and Butler, W. A.: Seasonal variations in elemental carbon aerosol, carbon monoxide and sulfur dioxide: Implications for sources, Geophys. Res. Lett., 28, 1711–1714, doi:10.1029/2000GL012354, 2001.

Chen, Y.: The impact of local circulation on the dirstribution and transport of atmospheric pollutants in Beijing, M.S. Thesis, Department of Atmospheric and Oceanic Sciences, Peking University, Beijing, 2009.

Chen, Y., Zhao, C., Zhang, Q., Deng, Z., Huang, M., and Ma, X.: Aircraft study of Mountain Chimney Effect of Beijing, China, J. Geophys. Res.-Atmos., 114, D08306, doi:10.1029/2008JD010610, 2009.

Deng, Z., Zhao, C., Zhang, Q., Huang, M., and Ma, X.: Statistical analysis of microphysical properties and the parameterization of effective radius of warm clouds in Beijing area, Atmos. Res., 93, 888–896, doi:10.1016/j.atmosres.2009.04.011, 2009.

Ding, A. J., Fu, C. B., Yang, X. Q., Sun, J. N., Zheng, L. F., Xie, Y. N., Herrmann, E., Nie, W., Petäjä, T., Kerminen, V. M., and Kulmala, M.: Ozone and fine particle in the western Yangtze River Delta: an overview of 1 yr data at the SORPES station, Atmos. Chem. Phys., 13, 5813–5830, doi:10.5194/acp-13-5813-2013, 2013.

Gao, X., Nie, W., Xue, L., Wang, T., Wang, X., Gao, R., Wang, W., Yuan, C., Gao, J., Ravi, K. P., Wang, J., and Zhang, Q.: Highly Time-Resolved Measurements of Secondary Ions in $PM_{2.5}$ during the 2008 Beijing Olympics: The Impacts of Control Measures and Regional Transport, Aerosol Air Qual. Res., 13, 367–376, doi:10.4209/aaqr.2012.04.0083, 2013.

He, S. Z., Chen, Z. M., Zhang, X., Zhao, Y., Huang, D. M., Zhao, J. N., Zhu, T., Hu, M., and Zeng, L. M.: Measurement of atmospheric hydrogen peroxide and organic peroxides in Beijing before and during the 2008 Olympic Games: Chemical and physical factors influencing their concentrations, J. Geophys. Res. Atmos., 115, D17307, doi:10.1029/2009JD013544, 2010.

Hua, W., Chen, Z. M., Jie, C. Y., Kondo, Y., Hofzumahaus, A., Takegawa, N., Chang, C. C., Lu, K. D., Miyazaki, Y., Kita, K., Wang, H. L., Zhang, Y. H., and Hu, M.: Atmospheric hydrogen peroxide and organic hydroperoxides during PRIDE-PRD'06, China: their concentration, formation mechanism and contribution to secondary aerosols, Atmos. Chem. Phys., 8, 6755–6773, doi:10.5194/acp-8-6755-2008, 2008.

Jacobson, M. Z.: Atmospheric Pollution: History, Science, and Regulation, Cambridge University Press, Cambridge, 2002.

Khemani, L. T., Momin, G. A., and Singh, G.: Variations in trace gas concentrations in different environments in India, Pure Appl. Geophys., 125, 167–181, doi:10.1007/BF00878620, 1987.

Lin, W., Xu, X., Zhang, X., and Tang, J.: Contributions of pollutants from North China Plain to surface ozone at the Shangdianzi GAW Station, Atmos. Chem. Phys., 8, 5889–5898, doi:10.5194/acp-8-5889-2008, 2008.

Lin, W., Xu, X., Ge, B., and Zhang, X.: Characteristics of gaseous pollutants at Gucheng, a rural site southwest of Beijing, J. Geophys. Res., 114, D00G14, doi:10.1029/2008jd010339, 2009.

Lin, W., Xu, X., Ge, B., and Liu, X.: Gaseous pollutants in Beijing urban area during the heating period 2007–2008: variability, sources, meteorological, and chemical impacts, Atmos. Chem. Phys., 11, 8157–8170, doi:10.5194/acp-11-8157-2011, 2011.

Lin, W., Xu, X., Ma, Z., Zhao, H., Liu, X., and Wang, Y.: Characteristics and recent trends of sulfur dioxide at urban, rural, and background sites in North China: Effectiveness of control measures, J. Environ. Sci., 24, 34–49, doi:10.1016/S1001-0742(11)60727-4, 2012.

Liu, H. J., Zhao, C. S., Nekat, B., Ma, N., Wiedensohler, A., van Pinxteren, D., Spindler, G., Müller, K., and Herrmann, H.: Aerosol hygroscopicity derived from size-segregated chemical composition and its parameterization in the North China Plain, Atmos. Chem. Phys. Discuss., 13, 20885–20922, doi:10.5194/acpd-13-20885-2013, 2013.

Liu, P. F., Zhao, C. S., Göbel, T., Hallbauer, E., Nowak, A., Ran, L., Xu, W. Y., Deng, Z. Z., Ma, N., Mildenberger, K., Henning, S., Stratmann, F., and Wiedensohler, A.: Hygroscopic properties of aerosol particles at high relative humidity and their diurnal variations in the North China Plain, Atmos. Chem. Phys., 11, 3479–3494, doi:10.5194/acp-11-3479-2011, 2011.

Madronich, S.: Chemical evolution of gaseous air pollutants downwind of tropical megacities: Mexico City case study, Atmos. Environ., 40, 6012–6018, doi:10.1016/j.atmosenv.2005.08.047, 2006.

Madronich, S. and Calvert, J. G.: Permutation reactions of organic peroxy radicals in the troposphere, Journal of Geophysical Research: Atmospheres, 95, 5697–5715, doi:10.1029/JD095iD05p05697, 1990.

Madronich, S. and Flocke, S.: The role of solar radiation in atmospheric chemistry, in: The Handbook of Environmental Chemistry, edited by: Boule, P., Springer-Verlag Berlin Heidelberg, 1–26, 1999.

OMSO2 Release Specific Information: http://so2.gsfc.nasa.gov/Documentation/OMSO2ReleaseDetails_v111_0303.htm, last access: 28 March 2013.

Pan, Y. P., Wang, Y. S., Tang, G. Q., and Wu, D.: Spatial distribution and temporal variations of atmospheric sulfur deposition in Northern China: insights into the potential acidification risks, Atmos. Chem. Phys., 13, 1675–1688, doi:10.5194/acp-13-1675-2013, 2013.

Pandis, S. N., Seinfeld, J. H., and Pilinis, C.: Heterogeneous sulfate production in an urban fog, Atmos. Environ., 26, 2509–2522, doi:10.1016/0960-1686(92)90103-R, 1992.

Psiloglou, B., Larissi, I., Petrakis, M., Paliatsos, A., Antoniou, A., and Viras, L.: Case studies on summertime measurements of O_3, NO_2, and SO_2 with a DOAS system in an urban semi-industrial region in Athens, Greece, Environ. Monitor. Assess., 185, 7763–7774, doi:10.1007/s10661-013-3134-2, 2013.

Qi, H., Lin, W., Xu, X., Yu, X., and Ma, Q.: Significant downward trend of SO_2 observed from 2005 to 2010 at a background station in the Yangtze Delta region, China, Sci. China Chem., 55, 1451–1458, doi:10.1007/s11426-012-4524-y, 2012.

Ran, L., Zhao, C. S., Xu, W. Y., Lu, X. Q., Han, M., Lin, W. L., Yan, P., Xu, X. B., Deng, Z. Z., Ma, N., Liu, P. F., Yu, J., Liang, W. D., and Chen, L. L.: VOC reactivity and its effect on ozone

production during the HaChi summer campaign, Atmos. Chem. Phys., 11, 4657-4667, doi:10.5194/acp-11-4657-2011, 2011.

Raymond, H. A., Yi, S.-M., Moumen, N., Han, Y., and Holsen, T. M.: Quantifying the dry deposition of reactive nitrogen and sulfur containing species in remote areas using a surrogate surface analysis approach, Atmos. Environ., 38, 2687–2697, doi:10.1016/j.atmosenv.2004.02.011, 2004.

Sakugawa, H., Tsai, W., Kaplan, I. R., and Cohen, Y.: Factors controlling the photochemical generation of gaseous H_2O_2 in the Los Angeles atmosphere, Geophys. Res. Lett., 17, 93–96, doi:10.1029/GL017i001p00093, 1990.

Slawson, P., and Csanady, G.: The effect of atmospheric conditions on plume rise, J. Fluid Mech., 47, 33–49, 1971.

Sun, M., Wang, Y., Wang, T., Fan, S., Wang, W., Li, P., Guo, J., and Li, Y.: Cloud and the corresponding precipitation chemistry in south China: Water-soluble components and pollution transport, J. Geophys. Res.-Atmos., 115, D22303, doi:10.1029/2010JD014315, 2010.

Tsai, J.-L., Chen, C.-L., Tsuang, B.-J., Kuo, P.-H., Tseng, K.-H., Hsu, T.-F., Sheu, B.-H., Liu, C.-P., and Hsueh, M.-T.: Observation of SO_2 dry deposition velocity at a high elevation flux tower over an evergreen broadleaf forest in Central Taiwan, Atmos. Environ., 44, 1011–1019, doi:10.1016/j.atmosenv.2009.12.022, 2010.

Wang, S., Hao, J., Ho, M. S., Li, J., and Lu, Y.: Intake fractions of industrial air pollutants in China: Estimation and application, Sci. Total Environ., 354, 127–141, doi:10.1016/j.scitotenv.2005.01.045, 2006.

Wang, T., Cheung, V. T. F., Lam, K. S., Kok, G. L., and Harris, J. M.: The characteristics of ozone and related compounds in the boundary layer of the South China coast: temporal and vertical variations during autumn season, Atmos. Environ., 35, 2735–2746, doi:10.1016/s1352-2310(00)00411-8, 2001.

Wang, T., Cheung, T. F., Li, Y. S., Yu, X. M., and Blake, D. R.: Emission characteristics of CO, NO_x, SO_2 and indications of biomass burning observed at a rural site in eastern China, J. Geophys. Res., 107, 4157, doi:10.1029/2001jd000724, 2002.

Wang, T., Wong, C. H., Cheung, T. F., Blake, D. R., Arimoto, R., Baumann, K., Tang, J., Ding, G. A., Yu, X. M., Li, Y. S., Streets, D. G., and Simpson, I. J.: Relationships of trace gases and aerosols and the emission characteristics at Lin'an, a rural site in eastern China, during spring 2001, J. Geophys. Res., 109, D19S05, doi:10.1029/2003JD004119, 2004.

Wang, T., Ding, A., Gao, J., and Wu, W. S.: Strong ozone production in urban plumes from Beijing, China, Geophys. Res. Lett., 33, L21806, doi:10.1029/2006gl027689, 2006.

Xu, W., Zhao, C., Ran, L., Deng, Z., Liu, P., Ma, N., Lin, W., Xu, X., and Yan, P.: Characteristics of Pollutants at a Suburban Site in the North China Plain and estimated regional Emissions and Contributions, AGU Fall Meeting Abstracts, 1, 0053, 2011a.

Xu, W. Y., Zhao, C. S., Ran, L., Deng, Z. Z., Liu, P. F., Ma, N., Lin, W. L., Xu, X. B., Yan, P., He, X., Yu, J., Liang, W. D., and Chen, L. L.: Characteristics of pollutants and their correlation to meteorological conditions at a suburban site in the North China Plain, Atmos. Chem. Phys., 11, 4353–4369, doi:10.5194/acp-11-4353-2011, 2011b.

Yang, D., Wang, Z., and Zhang, R.: Estimating Air Quality Impacts of Elevated Point Source Emissions in Chongqing, China, Aerosol Air Qual. Res., 8, 279–294, doi:10.4209/aaqr.2008.02.0005, 2008.

Zhao, P. S., Dong, F., He, D., Zhao, X. J., Zhang, X. L., Zhang, W. Z., Yao, Q., and Liu, H. Y.: Characteristics of concentrations and chemical compositions for $PM_{2.5}$ in the region of Beijing, Tianjin, and Hebei, China, Atmos. Chem. Phys., 13, 4631–4644, doi:10.5194/acp-13-4631-2013, 2013.

Zhou, Y., Levy, J. I., Hammitt, J. K., and Evans, J. S.: Estimating population exposure to power plant emissions using CALPUFF: a case study in Beijing, China, Atmos. Environ., 37, 815–826,